Kulig et al.*Chemistry and Physics of Lipids* **2016,** *195*, 12-20.
http://dx.doi.org/10.1016/j.chemphyslip.2015.07.002

# C*is* and *Trans* Unsaturated Phosphatidylcholine Bilayers: A Molecular Dynamics Simulation Study

**Waldemar Kulig†, Marta Pasenkiewicz-Gierula‡, T. Róg†**

AUTHOR EMAIL ADDRESS tomasz.rog@gmail.com, tomasz.rog@tut.fi

CORRESPONDING AUTHOR FOOTNOTE Tel.: +358 40 198 1010. Fax: +358 3 3115 3015. E-mail: tomasz.rog@tut.fi (T.R.).

† Department of Physics, Tampere University of Technology, PO Box 692, FI-33101 Tampere, Finland

‡ Faculty of Biochemistry, Biophysics and Biotechnology, Jagiellonian University, ul. Gronostajowa 7, 30-387 Kraków, Poland

Kulig et al.*Chemistry and Physics of Lipids* **2016,** *195*, 12-20.
http://dx.doi.org/10.1016/j.chemphyslip.2015.07.002

## ABSTRACT

*Trans* unsaturated lipids are uncommon in nature. In the human diet, they occur as natural products of ruminal bacteria or from industrial food processing like hydrogenation of vegetable oils. Consumption of *trans* unsaturated lipids has been shown to have a negative influence on human health; in particular, the risk of cardiovascular disease is higher when the amount of *trans* unsaturated lipids in the diet is elevated. In this study, we first performed quantum mechanical calculations to specifically and accurately parameterize *cis* and *trans* mono-unsaturated lipids and subsequently validated the newly derived parameter set. Then, we carried out molecular dynamics (MD) simulations of lipid bilayers composed of *cis* or *trans* unsaturated lipids with and without cholesterol. Our results show that *trans* mono-unsaturated chains are more flexible than *cis* mono-unsaturated chains due to lower barriers for rotation around the single bonds next to the *trans* double bond than those next to the *cis* double bond. In effect, interactions between cholesterol and *trans* unsaturated chains are stronger than *cis* unsaturated chains, which results in a higher ordering effect of cholesterol in *trans* unsaturated bilayers.

**Keywords:** cholesterol; OPLS-AA force field; torsional potential; model validation

## Graphical Abstract:

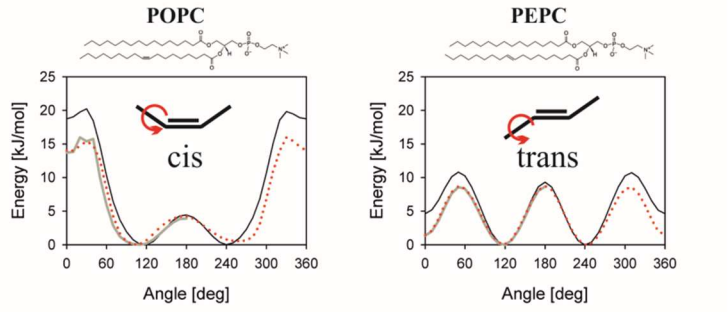


**Highlights:**

- New force-field parameters were derived and validated for *cis* and *trans* unsaturated double bonds.
- Chains containing *trans* double bonds are more flexible due to the free rotation around saturated bonds next to the unsaturated one.
- Cholesterol affects *trans* unsaturated lipids more than *cis* unsaturated but less than saturated.

# 1. INTRODUCTION

Cholesterol is a major component of animal cell membranes. It strongly influences physical properties of the lipid matrix of biomembranes, such as permeability, mechanical strength, and phase state (Ohvo-Rekilä et al., 2002). At the molecular level, the order of hydrocarbon chains, surface area per lipid and thickness of the matrix are regulated by the cholesterol content (Róg et al., 2009); consequently, cholesterol affects interactions of integral membrane proteins with membrane lipids (Song et al., 2014). Cholesterol governs interactions between lipid head groups and sodium ions (Magarkar et al., 2014) as well as interactions between peripheral membrane proteins and the membrane surface (Lingwood et al., 2011). For these reasons, cholesterol interactions with various lipid classes present in animal cell membranes like phosphatidylcholines (PC) and sphingomyelins are intensively studied (Róg and Vattulainen, 2014). Among PCs, the most frequently occurring in nature are those with *cis* unsaturated acyl chains (*cis* unsaturated lipids). As such they, as well as PCs with saturated acyl chains, are the most commonly used in biophysical studies of the effect of cholesterol on the properties of model membranes. In contrast, similar studies on *trans* unsaturated lipids are infrequent, e.g., (Róg et al., 2004), mainly because *trans* fatty acids are rather rare in nature. However, as we explain below, their impact on human health certainly justifies our interest in cholesterol interactions with this class of lipids.

*Trans* unsaturated lipids occur in photosynthetic membranes of algae and higher plants (Dubertret et al., 1994; Ohnishi and Thompson, 1991) as well as in bacteria (Gillan et al., 1981) In humans, free radical-catalyzed *cis-trans* isomerization of unsaturated lipids is an endogenous source of these lipids (Chatgilialoglu and Ferrari, 2005). In natural human diet, *trans* unsaturated lipids occur in small quantities, mainly in dairy products originating from ruminant bacteria, but, currently, 90% of *trans* unsaturated lipids in diet come from hydrogenated oils (Jala et al., 2013). The most common *trans* fatty acids are elaidic acid (18:1 10t) (Schofield et al., 1967) generated during hydrogenation of vegetable oils and vaccenic acid (18:1 11t) (Hay and Morrison, 1970)

naturally present in milk and its products. Amount of *trans* unsaturated acids consumed in industrialized countries is estimated to be 2–8% of all fatty acids providing 2.5% of total energy (Larque et al., 2001). Epidemiological studies clearly associate high diet content of *trans* fats with an increased risk of cardiovascular disease. For example, a 2% increase of total energy originating from *trans* fats leads to a 23% increase in cardiovascular risk. A factor which might contribute to the enhancement of cardiovascular risk is an increase of the blood level of low-density lipoprotein (LDL) associated with a decreased level of high-density lipoprotein (HDL) (Uauy et al., 2009). *Trans* fats increase production of proinflammatory cytokines (Ganguly and Pierce, 2012). This may play a role in development of diabetes, atherosclerosis, and plague rapture. *Trans* unsaturated lipids were also shown to affect membrane protein functions, e.g., they decrease the activation level of rhodopsin (Niu et al., 2005) but increase the activity of cholesteryl-ester transfer protein (van Tol et al., 1995). Negative health effects of *trans* unsaturated lipids are independent of their source, either natural or industrial (Brouwer et al., 2010).

Lipids with *trans* unsaturated acyl chains are components of cell membranes of specific bacteria like *pseudomonads*, *vibrios* and *methylotrophs* where they play important physiological functions similar to *cis* unsaturated or saturated lipids (Keweloh and Heipieper, 1996). One of the functions of *trans* unsaturated lipids is associated with bacterial response to higher temperature as the content of *trans* fatty acids increases with temperature (Jogadhenu and Prakash, 2010; Cronan, 2002; Heipieper et al., 1996; Okuyama et al., 1991; Morita et al., 1993). The main phase transition temperature of *trans* unsaturated lipids is known to be higher than that of analogical *cis* isomers (Koynova and Caffrey, 1998), thus their presence decreases membrane fluidity at a given temperature and can serve as an adaptive mechanism (Keweloh and Heipieper, 1996). Concentration of *trans* unsaturated lipids in membranes is controlled by single enzyme *cis*→*trans* isomerase (Holtwick et al.,1997). This enzymatic mechanism, which was shown to occur in e.g., *E. coli* in response to the temperature rise, was much faster than *de*

*novo* synthesis of *trans* unsaturated lipids (de Mendoza and Cronan, 1983). Increased membrane concentration of *trans* unsaturated lipids was also shown to be an adaptive mechanism used by bacteria in response to organic solvents; it is because their presence elevates stability and decreases permeability of bacterial membranes (Segura et al., 2012; Torres et al., 2011; Bernal et al., 2007; Heipieper et al., 2003; Sardessa and Bhosle, 2002; Junker and Ramos, 1999; Heipeiper et al., 1996; Weber et al., 1994; Moritaet al., 1993).

Biophysical studies on model membranes indicate that bilayers consisting of *trans* mono-unsaturated lipids have properties intermediate between those consisting of saturated and *cis* mono-unsaturated lipids (Róg et al., 2004; Vollhardt, 2007; Pearce and Harvey, 1993). This concerns the main phase transition temperature (Tm), which for t18:1-18:0PC is 31.5 °C, while for c18:1-18:0PC and 18:0-18:0PC is 7 and 53 °C, respectively (Soni et al., 2009). Also ordering of hydrocarbon chains above Tm (Soni et al., 2009) and lateral mobility of *trans* unsaturated lipids are intermediate between saturated and *cis* unsaturated lipids (Roach et al., 2004). Bilayers formed of *trans* unsaturated lipids were shown to be less fluid and less permeable than those of *cis* unsaturated lipids (Moss et al., 1991). The *cis* double bond greatly increases hydrophobicity of the bilayer core; the effect is weaker in the case of the *trans* double bond (Subczynski et al., 1991). Cholesterol has higher affinity towards *trans* unsaturated phospholipids than corresponding *cis* unsaturated lipids (Niu et al., 2005). In quaternary bilayers consisting of *cis* and *trans* unsaturated PCs, saturated lipids, and cholesterol, *trans* unsaturated lipids formed sterol rich domains together with saturated lipids. But at lower temperatures, they formed such domains even without the presence of saturated lipids (Björkbom et al., 2007). Another study demonstrated that *trans* unsaturated N-elaidoyl-sphingomyelin and cholesterol made so-called detergent-resistant membrane domains while *cis* unsaturated N-oleoyl-sphingomyelin had no such ability. However, domains formed by *trans* unsaturated sphingomyelins were smaller than those of saturated sphingomyelin (Waarts et al., 2002).

The aim of this study was to compare the effect of cholesterol on *trans* and *cis* mono-unsaturated phospholipids in the hydrated bilayer using molecular dynamics simulations. In the first step, we parameterized separately *cis* and *trans* unsaturated hydrocarbons by recalculating torsional potential of the single bonds next to the unsaturated bond and of the two following single bonds. The obtained rotational energy profiles for the single bonds next to the double bond differed significantly between the *cis* and *trans* bonds. In the next step, we validated our model of unsaturated chains in the condense phase and in bilayers against existing experimental data. Our study demonstrated that acyl chains with the *trans* double bond are more flexible than those with the *cis* double bond. This is a result of higher rotational freedom of the single bonds next to the *trans* double bond. Greater flexibility of chains facilitates their better packing in the bilayer, thus, the order of *trans* unsaturated chains in bilayers is higher than *cis* unsaturated and their interactions with cholesterol are stronger.

# 2. METHODS

### 2.1 Simulated Models

In this work, we performed molecular dynamics simulations of pure hydrocarbons, *cis*/*trans*-3-decene and *cis*/*trans*-5-decene, in the condense phase. The initial structure of each simulation system consisted of 200 molecules randomly placed in the simulation box. We also simulated bilayers consisting of 1,2-dioleoyl-phosphatidylcholine (DOPC), 1-palmitoyl-2-oleoyl-phosphatidylcholine (POPC), 1-palmitoyl-2-elaidoyl-phosphatidylcholine (PEPC) and their binary mixtures with 20 mol% cholesterol (CHOL). A detailed list of simulated bilayers is given in Table 1. The initial structures of the bilayers originated from our previous studies (Stępniewski et al., 2012). All bilayers were composed of 128 PC molecules and mixed PC-CHOL bilayers included additionally 32 cholesterol molecules. 6400 water molecules were used to hydrate the bilayers. Chemical structures of all molecules are shown in Figure 1.

### 2.2 Force Field

For the PC molecules, we used parameters derived in our previous studies for DPPC (Maciejewski et al., 2014) that are compatible with the OPLS-AA force field (Jorgensen et al., 1996; Kaminski et al., 2001) as well as new parameters for *cis* and *trans* mono-unsaturated hydrocarbons derived in this study. The set of parameters for DPPC includes parameters for saturated hydrocarbon chains, glycerol backbone, and phosphatidylcholine head group. For cholesterol, we used original OPLS-AA force-field parameters; their compatibility with the new parameters for *cis* and *trans* hydrocarbons was tested in this study. For water, we used TIP3P model (Jorgensen et al., 1983) compatible with OPLS-AA. Topologies of all lipids, parameters, and corresponding structures can be found in supporting information in the GROMACS format.

New torsional parameters were calculated for the *cis* and *trans* double bond (CM0) and two subsequent single bonds (CM1 and CM2) in 3-decene and 5-decene (see Figure 1). Bond stretching, angle bending, and partial atomic charges, and also Lenard-Jones parameters for sp2 carbon atoms were as they were in the original OPLS-AA force field. For sp3 carbon atoms, Lenard-Jones parameters derived for long saturated hydrocarbons in our previous study were used (Maciejewski et al., 2014, section 2.1.4 „Hydrocarbon Chain Parameterization"). The protocol for deriving torsional potential was the same as in Ref. (Maciejewski et al., 2014). In these calculations profile of torsional energy was scanned every 10°. Energy evaluation was done using the Hybrid Methods for Interaction Energies (HM-IE) (Klauda et al., 2004; Klauda et al., 2005). All electronic structure calculations were carried out using the GAUSSAN-03/09 suite (Frisch et al., 2004).

### 2.3 Simulation Protocol

All MD simulations were performed using GROMACS package (version 4.6) (Hess et al., 2008). For each bilayer, a single 300-ns MD simulation was run with the first 50 ns considered

equilibration and the last 250 ns the production simulation—the latter trajectory fragment was used for analysis. The LINCS algorithm was applied to preserve the lengths of all covalent bonds allowing for 2-fs time step (Hess et al., 1997). Simulations were carried out in the isobaric-isothermal ensemble under a constant pressure of 1 atm and a semi-isotropic pressure control. Temperatures of all simulated systems are given in Table 1. The temperature and pressure were controlled using the Nosé-Hoover (Nose, 1984; Hoover, 1985) and the Parrinello-Rahman (Parrinello and Rahman, 1981) algorithms, respectively. The temperatures of the solute and solvent were controlled independently. The list of non-bonded pairs was updated every 10 steps using grid algorithm. The van der Waal interactions were cut off at 10 Å. Dispersion corrections for both energy and pressure were used in order to remove dependencies on the cut-off length and to keep the model compatible with the OPLS-AA force field. The electrostatic interactions were evaluated using the particle-mesh Ewald (PME) summation (Essman et al., 1995) with β-spline interpolation order of 6, and direct sum tolerance of $10^{-6}$. For the real space, a cut-off of 10 Å, periodic boundary conditions, and the usual minimum image convention were used.

**2.4 Analysis**

The surface area per lipid in a single component bilayer was obtained by dividing the area of the bilayer by the number of lipid molecules in one leaflet. The surface area per PC in mixed PC-CHOL bilayers was obtained by subtracting the cross-sectional area of CHOL molecules from the total surface area of the bilayer and then dividing it by the number of PC molecules present in one leaflet. The mean surface area of the CHOL molecule of 0.39 $nm^2$ was determined in an experimental study on a CHOL monolayer (Hyslop et al., 1990) and of 0.380 ± 0.002 $nm^2$ in an MD simulation study of a CHOL bilayer (Plesnar et al., 2912). Bilayer thickness was approximated by a so-called P-P distance—the distance between average positions of phosphorous atoms in the opposite bilayer leaflets. Tilt of a CHOL molecule was

calculated as an angle between the vector connecting carbon atoms C3 and C17 (c.f. Fig. 1) and the bilayer normal. Tilt of an acyl chain was calculated as an angle between the vector connecting the first and the last carbon atoms of the chain and the bilayer normal. Tilt of the upper part of the unsaturated chain (above the double bond, V1) was calculated for the vector connecting the first carbon atom of the chain and the first carbon atom of the double bond (C9), and that of the lower part of the unsaturated chain (below the double bond, V2) was calculated for the vector connecting the second carbon atom of the double bond (C10) and the last carbon in the chain. The deuterium order parameter, $S_{CD}$, is a bilayer parameter that provides information about the chain's order (Davis, 1983). It can be obtained accurately from NMR experiments. $S_{CD}$ is defined as:

**Eq. 1**. $$S_{CD} = \left\langle \frac{3}{2}\left(\cos^2 \theta i\right) - \frac{1}{2} \right\rangle$$

where $\theta_i$ is the angle between a C-D bond (C-H in simulations) of the *i*-th carbon atom and the bilayer normal. The angular brackets denote averaging over time and over relevant C-D bonds in the bilayer.

The form factor, $F(q)$ (Eq. 2), computed from simulations can be compared to experimental "model-free" measurements. To get $F(q)$, first, the relative electron density profile $\rho_r(z)$ has to be computed by subtracting the electron density of bulk water from that of the total bilayer system. The X-ray scattering form factor is then calculated as (Kucerka 2006):

**Eq. 2.** $$|F(q)| = \sqrt{\left(\int_{-L/2}^{L/2} \rho_r(z)\cos(qz)dz\right)^2 + \left(\int_{-L/2}^{L/2} \rho_r(z)\sin(qz)dz\right)^2}$$

where $L$ is the length of the simulation box in the $z$ direction. In these calculations electron density was calculated with Gromacs analysis tools while the form factor was obtained using in-house code. Radial distribution function (RDF) describes the probability of finding a particle $\beta$ at a distance between $r$ and $r+dr$ away from a particle $\alpha$ in a simulation box of the volume $V$ containing $N$ particles:

**Eq. 3.** $$RDF = \frac{V}{N}\left\langle \frac{n(r)}{4\pi r^2 dr} \right\rangle$$

where *n(r)* is the number of particles β in the spherical ring of radius *r* and width *dr* around the particle α, and $4\pi r^2 dr$ is the ring volume; $\langle\ \rangle$ denotes the time and ensemble average. Definitions of polar interactions (H bonds and charge pairs) were based on geometrical criteria derived in our previous study (Pasenkiewicz-Gierula et al., 1999; Murzyn et al., 2001). H bond was judged to be formed when the acceptor-donor distance is ≤ 0.325 nm and the angle between the acceptor···donor vector and the covalent bond donor-hydrogen is ≤ 35°. A charge pair is formed between a positively charged choline methyl group and negatively charged oxygen atoms when they are located within 4.0 Å from each other.

# 3. RESULTS

### 3.1 Unsaturated hydrocarbon parameterization and validation

Rotational energy profiles for torsion angles CM0, CM1, and CM2 (see Figure 1) in *cis* and *trans* 3-decene are shown in Figure 2. The fitted Ryckaert-Bellemans (RB) coefficients are given in Table 2 and in Supplementary Information in the Gromacs format. As can be seen in Figure 2c and d, there are substantial differences between the profiles for a single bond next to the *cis* and to the *trans* double bond (CM1, Figure 1), whereas for the following single bond, there are no apparent differences.

In the first step of validation of the new torsional parameters, we performed MD simulations of pure *cis*/*trans*-3-decene and *cis*/*trans*-5-decene. In these simulations, the same simulation protocol as described in the Methods section was used with the following alternations: simulation temperature was 298.15 K; equilibration stage was 10 ns; and analysis was performed for 15-ns production runs. Densities of both 3-decene and 5-decene obtained in these simulations differ less than 1% from experimental values; thus, the agreement between

simulation and experiment is very good (Table 3). However, for the heat of vaporization, the discrepancy between simulation and experiment is larger and up to 17%.

In the next step, we validated the model of the whole *cis* unsaturated lipid molecule in MD simulations of hydrated bilayers consisting of POPC and DOPC. Profiles of the deuterium order parameter, $-S_{CD}$, for both chains of POPC obtained in these simulations and measured experimentally (Mendes Ferreira et al., 2013) are shown in Figure 3. In both simulated and experimental bilayers, ordering of acyl chains is similar; however, small differences in the upper segments of both chains are observed. Absolute form factors for the POPC and DOPC bilayers obtained in these MD simulations are compared with those obtained in experiments (Kučerkaa et al., 2009, 20011) in Figure 4. The agreement between both sets of data is very good which indicates that the area per lipid and the thickness of both bilayers are correct.

To accomplish comparison between *cis* and *trans* unsaturated chains, we calculated probability of population of torsion angles neighboring the double bond, and the distributions of probabilities are shown in Figure 5. Calculations were performed on POPC and PEPC bilayers. For the *cis* unsaturated bond, the distribution has two maxima at 120 and -129°, while for the *trans* unsaturated bond an additional maximum at 0° is present. Rotation about the single bonds next to the *cis* double bond is restricted to the range of angles between 60 and 300° (–60°) (Figure 5), while for the *trans* double bond, rotation is not restricted, which indicates that the chain with the *trans* double bond is more flexible.

### 3.2 Comparison *cis* and *trans* unsaturated lipids and cholesterol effects on their properties.

First, we calculated standard properties characterizing lipid bilayers: the area per lipid molecule, the bilayer thickness, and the order parameter profile of the acyl chains, $-S_{CD}$. For the POPC and PEPC bilayers, the values for the area and thickness are given in Table 4, and the profiles are shown in Figure 6. The area per PEPC is smaller of about 0.02 $nm^2$ than per

POPC in single component bilayers (Table 4). Consistently with this result, the order of the PEPC acyl chains is higher than that of the POPC chains (Figure 6). Also, thickness of the PEPC bilayer is slightly larger than that of the POPC bilayer (Table 4). These results agree well with experimental and theoretical data discussed in the Introduction. The condensation and ordering effects of CHOL on acyl chains are greater in the PEPC than POPC bilayers, which also agrees with the literature data discussed in the *Introduction*.

Next, we analyzed the tilt of the acyl chains, the lower and upper parts of the unsaturated *sn*2 chains, and the CHOL rings. Average values of tilts are given in Table 4. In all cases, tilts for the PEPC bilayer are smaller than those for the POPC bilayer. As tilt of the acyl chains is inversely correlated with their order parameter, the order is higher in the PEPC than POPC bilayers, and it is further increased by the presence of cholesterol, as can be seen from Figure 6. The increase concerns both *sn*1 and *sn*2 chains. Tilt of the sterol ring was shown to correlate with the magnitude of its condensing and ordering effects (Aittoniemi et al., 2006). In the studied systems, the average tilt of CHOL is independent on the conformation of the double bond and is in the errors range in the PEPC and POPC bilayers (Table 4). This means that correlation between sterol tilt and sterol condensing and ordering effects does not necessarily occur for all lipids present in the lipid matrix of biomembranes, however, this result might be due to the limited accuracy of the calculations. Distributions of cholesterol tilt angles are very similar in both bilayer types (data not shown).

Position of the hydroxyl group of CHOL was shown to correlate with the magnitude of its ordering and condensing effects in a saturated PC bilayer (Róg and Pasenkiewicz-Gierula, 2003). The mass density profiles across one bilayer leaflet for the PC phosphorous atoms and the oxygen atoms of CHOL in the PEPC-CHOL bilayer overlap with those in the POPC-CHOL bilayer (Figure 7); thus, the CHOL oxygen atoms in both bilayers are located in equivalent positions.

A weaker ordering effect of CHOL in mono-unsaturated bilayers compared to saturated ones has been often associated with the stiffness of the double bond that fits worse with the rigid cholesterol ring. In fact, distributions shown in Figure 5 imply that chains with the *cis* double bond are more rigid compared to those with the *trans* double bond. It is because the single bonds next to the *trans* double bond can rotate more freely (there are no unpopulated torsion angles) than those next to the *cis* double bond (torsion angles between 300 and 60° are not populated). To evaluate interactions between the double bond and the CHOL ring, we calculated the radial distribution function (RDF) of the CHOL methyl groups C18 and C19 (cf. Figure 1), as well as the carbon atoms of the unsaturated bond of PC in the PEPC-CHOL and POPC-CHOL bilayers. The RDF curves shown in Figure 8 have complex structure due to asymmetry of the sterol ring (Róg and Pasenkiewicz-Gierula, 2004), but they clearly indicate stronger interaction between CHOL and the *trans* unsaturated bond. To evaluate differences between interaction of *cis* and *trans* unsaturated bonds with CHOL in a more quantitative term, we calculated the number of neighbors, that is the number of the double bond carbon atoms at the distance less than 0.7 nm (approximate sum of van der Waals radii of two carbon atoms, corresponding to the position of the first minimum of the carbon-carbon RDF of acyl chains) from a CHOL molecule (Table 4). The number of neighbors in the POPC bilayer is about 3.5% smaller than in the PEPC bilayer. In our previous study, we showed that the location of the double bond at position 9–10 leads to the weakest interaction of the bond with CHOL compared to any other location along the acyl chain (Martinez-Seara et al., 2008). This location overlaps with that of the CHOL methyl groups C18 and C19, which, to a large extent, affect the ordering and condensing capability of CHOL (Róg et al., 2007; Krause et al., 2014). To demonstrate these overlaps, we calculated the mass density profile along the bilayer normal of the double bond carbon atoms and the CHOL methyl groups C18 and C19 in the PEPC-CHOL and POPC-CHOL bilayers, and they are shown in Figure 9. Indeed, the overlap is clear. Additionally, the distributions of the *cis* double bond

carbon atoms are broader as they extend more toward the water phase and the bilayer center, and are not symmetric.

Finally, we analyzed CHOL-PC interactions at the bilayer/water interface. We calculated the number of CHOL-PC hydrogen bonds, CHOL-water hydrogen bonds, and CHOL-PC charge pairs (between the CHOL oxygen atom and positively charged choline methyl groups) using definitions derived in our previous studies (Pasenkiewicz-Gierula et al., 1999; Murzyn et al., 2001). The numbers are given in Table 5, and they show that the patterns of interactions between CHOL and both *cis* and *trans* unsaturated PC as well as water are very similar.

## 4. CONCLUSIONS

The aim of this study was to faithfully parameterize the *cis* and *trans* double bonds and the single bonds in their close neighborhood using quantum mechanics calculations and to validate the developed parameter set. Parameterization was tested first on fragments of a lipid molecule, specifically on *cis*- and *trans*-decanes, giving close agreement with experimental data for density and heat of vaporization (Table 3). Next, we performed validation of a whole lipid molecule for two *cis* mono-unsaturated lipid species, DOPC and POPC, in bilayers. For DOPC and POPC, there are experimental data (NMR order parameter profiles and form factors obtained in neutron scattering experiments) obtained from direct measurements that can be compared with simulation results (Figures 3 and 4). This comparison showed very good agreement between simulations and experiments in the case of form factors indicating that the area per lipid and the bilayer thickness are reproduced correctly in simulations. In the case of $S_{CD}$ profiles, the agreement is generally good, but there are small deviations for some chain segments.

Quantum mechanics calculations reveal that the barriers for rotation around a single bond next to the *trans* double bond are ~30% lower than those next to the *cis* double bond (Figure 2). This results in more free rotation around this bond (Figure 5) and subsequently in higher flexibility of the whole chain. In effect, the order of the *trans* mono-unsaturated chains in the

bilayer is higher than *cis*. This agrees with experimental (Subczynski et al., 1991; Waarts et al., 2002; Roach et al., 2004; Björkbom et al., 2007; Soni et al., 2009) and other MD simulation data (Pearce and Harvey, 1993; Róg et al., 2004; Roach et al., 2004; Soni et al., 2009), indicating that *trans* unsaturated bonds have properties intermediate between *cis* unsaturated and saturated chains; also, it agrees with a biological function of *trans* unsaturated fats as regulators of membrane fluidity in bacteria e.g. (Heipeiper et al., 1996; Weber et al., 1994).

Cholesterol is known to increase the order of both saturated and mono-unsaturated acyl chains; however, this effect is stronger in the case of saturated chains (Róg and Vattulainen, 2014). Our results show that the CHOL ordering effect is stronger for *trans* than *cis* unsaturated lipids (Figure 6), but when compared with the CHOL effect on saturated lipids shown in our previous studies, it is again intermediate between *cis* unsaturated and saturated lipids (Kulig et al., 2014). Polar interactions between CHOL and head groups of *trans* and *cis* unsaturated PCs are the same within the error range (Table 5); also, position of the CHOL hydroxyl group in the bilayer/water interface is the same (Figure 7). Additionally, CHOL tilt does not differentiate between these lipid types (Table 4). The only difference in the CHOL interactions with POPC and PEPC concerns the non-poplar bilayer core where the number of neighbors of the *trans* unsaturated bond is greater compared to that of the *cis* unsaturated bond (Figure 8, Table 4). This difference can be explained by higher flexibility of *trans* unsaturated chains, which allows for better packing of more flexible chains next to the rigid, inflexible cholesterol ring.

Differences between properties of bilayers composed of *cis* and *trans* unsaturated phospholipids and differences in the phospholipids interactions with cholesterol might explain reduced activation of rhodopsin observed experimentally (Niu et al., 2005). Rhodopsin belongs to the family of G-protein coupled receptors which are known to interact and depend on cholesterol (Róg and Vattulainen, 2014) thus changes in affinity of cholesterol to the membrane lipids might be of high importance.

**ACKNOWLEDGMENTS**. We wish to thank the Academy of Finland (Center of Excellence in Biomembrane Research), and the European Research Council (Advanced Grant project CROWDED-PRO-LIPIDS) for financial support. For computational resources, we wish to thank the CSC–IT Center for Science, Espoo, Finland (project number tty3995). We thank Arkadiusz Maciejewski for performing QM calculations of rotational energy profiles and fitting torsional potentials.

**Supporting Information Available:** POPC, DOPC, and PEPC molecules in Gromacs format with all necessary parameters files and structure of lipid bilayer in GRO format.

**Figure Captions:**

**Figure 1.** Chemical structures of molecules and molecular fragments used in this study.

**Figure 2**. Profiles of the torsional energy for the double bond (CM0) (a, b), single bond next to the double bond (CM1) (c, d), and second single bond (CM2) (e, f) for *cis* double bond (a, c, e) and *trans* double bond (b, d, f). Results obtained with HM-IE method are shown as solid gray line and fits used in atomistic model are shown as red doted line. For comparison, profile obtained with Hartree-Fock (HF) -level calculations with 6-31G*basis set is shown. Since all profiles are symmetric, HM-IE calculations were performed for half of the angle range.

**Figure 3**. Profiles of the $-S_{CD}$ parameter for the *sn*-2 (a) and *sn*-1 (b) chains of POPC obtained in MD simulation (black line) and from experimental data (from Ref. (Mendes Ferreira et al., 2013) (red line) at 300 K.

**Figure 4**. Absolute form factors as a function of wave number q for POPC bilayer at 313 K (a) and DOPC at 300 K (b). Result of MD simulations – black line, experimental result – red dots. Experimental data are from Refs. (Kučerkaa et al., 2009, 2011) for POPC and DOPC, respectively.

**Figure 5**. Distribution of probability of population of torsion angles for a single bond next to the double bond (CM1) in the *cis* unsaturated (POPC) (black line) and the *trans* unsaturated (PEPC) (red line) bilayers.

**Figure 6**. Profiles of the $-S_{CD}$ parameter for the *sn*-2(b) and *sn*-1 (a) chains of POPC (blac line) and PEPC (red line) in bilayers with 0 (solid line) and 20 mol% (dashed line) cholesterol at 310K. Experimental data from (Seelig and Nada Waespe-Sarcevit, 1978) for PEPC at 313K shown as squares.

**Figure 7.** Mass density profiles along the bilayer normal of the phosphorous atoms of PC (solid line) and the oxygen atoms of CHOL (dashed line) in the PEPC-CHOL (red line) and POPC-CHOL (black line) bilayers.

**Figure 8.** Radial distribution function (RDF) of the PC double-bond carbon atoms C9 and C10 relative to the carbon atoms of the CHOL methyl groups C18 and C19 in the POPC (black line) and PEPC (red line) bilayers.

**Figure 9.** Mass density profile along the bilayer normal of cholesterol methyl groups C19 (red line) and C18 (blue line) and carbon atoms of the unsaturated bond of PC, C9 (green line) and C10 (black line), in the PEPC-CHOL (a) and POPC-CHOL (b) bilayers.

## References:

Aittoniemi, J., Róg, T., Niemelä, P.S., Pasenkiewicz-Gierula, M., Karttunen, M., Vattulainen, I., 2006. Tilt: major factor in sterols' ordering capability in membranes. J. Phys. Chem. B 110, 25562-25564.

Bernal, P, Segura, A, Ramos, J.L. 2007. Compensatory role of the cistrans-isomerase and cardiolipin synthase in the membrane fluidity of *Pseudomonas putida* DOT-T1E. Environ. Microbiol. 9, 1658–1664.

Björkbom, A., Ramstedt, B., Slotte, J.P. 2007. Phosphatidylcholine and sphingomyelin containing an elaidoyl fatty acid can form cholesterol-rich lateral domains in bilayer membranes. Biochim. Biophys. Acta 1768, 1839–1847.

Brouwer, I.A., Wanders, A.J., Katan, M.B. 2010. Effect of animal and industrial trans fatty acids on HDL and LDL cholesterol levels in humans – A quantitative review. PLoS ONE 5, e9434.

Chatgilialoglu C. Ferrari A. 2005. Trans lipids: The free radical path. Accounts Chem. Res. 38, 441–448.

Cronan, Jr, J.E. 2002. Phospholipid modifications in bacteria. Curr. Opinion Microbiol. 5, 202–205.

Davis, J.H. 1983. The description of membrane lipid conformation, order and dynamics by $^{2}$H-NMR. Biochim. Biophys. Acta, 737, 117−171.

de Mendoza, D., Cronan, J.E. Jr: 1983. Temperature regulation of membrane fluidity in bacteria. Trends Biochem. Sci. 8, 49–52.

Dubertret, G., Mirshahi, A., Mirshahi, M., Gerard-Hirne, C., Tremolieres, A. 1994. Evidence from *in vivo* manipulations of lipid composition in mutants that the _3-*trans*-hexadecenoic acid-containing phosphatidylglycerol is involved in the biogenesis of the light-harvesting chlorophyll *a/b*-protein complex of *Chlamydomonas reinhardtii*. Eur. J. Biochem. 226, 473–482.

Essman, U., Perera, L., Berkowitz, M.L., Darden, H.L.T., Pedersen, L.G. 1995. A smooth particle mesh Ewald method. J. Phys. Chem. 103, 8577−8592.

Frisch, M.J., Trucks, G.W., Schlegel, H.B., Scuseria, G.E., Robb, M.A., Cheeseman, J.R., Montgomery, J.A., Vreven, T., Jr., Kudin, K.N., Burant, J.C. et al. Gaussian 03, Revision C.02, Gaussian, Inc., Wallingford CT, 2004.

Ganguly, R., Pierce, G. N. 2012. Trans fat involvement in cardiovascular disease. Mol. Nutr. Food Res. 56, 1090–1096.

Gillan, F.T., Johns, R.B., Verheyen, T.V., Volkman, J.K., Bavor, H.J. 1981. *Trans*-monounsaturated acids in a marine bacterial isolate. Appl. Environ. Microbiol. 41, 849–856.

Hay, H.D., Morrison, W.R. 1970. Isomeric monoenoic fatty acids in bovine milk fat. Biochim. Biophys. Acta 202, 237–243.

Haynes, W.M. Ed. 2014. CRC handbook of chemistry and physics, 98$^{th}$ edition. CRC Press.

Heipeiper, H., Meulenbeld, G., van Oirschot, Q., de Bont, J. 1996. Effect of environmental factors on the trans-cis ratio of unsaturated fatty acids in Pseudomonas putida S12. Appl. Environ. Microbiol. 62, 2773– 2777.

Heipieper, H.J., Meinhardt, F., Segura, A. 2003. The cis–trans isomerase of unsaturated fatty acids in Pseudomonas and Vibrio: biochemistry, molecular biology and physiological function of a unique stress adaptive mechanism. FEMS Microbiol Lett, 229, 1–7.

Heipieper, H.J., Meulenbeld, G., van Oirschot, Q., de Bont, J.A. 1996. Effect of environmental factors on the *trans/cis* ratio of unsaturated fatty acids in *Pseudomonas putida* S12. Appl. Environ. Microbiol. 62, 2773–2777.

Hess, B., Bekker, H., Berendsen, H.J.C., Fraaije, J.G.E.M. 1997. LINCS: A linear constraint solver for molecular simulations. J. Comput. Chem., 18, 1463−1472.

Hess, B., Kutzner, C., van der Spoel, D., Lindahl, E. 2008. GROMACS 4: Algorithms for Highly Efficient, Load-Balanced, and Scalable Molecular Simulation. J. Chem. Theory Comput. 4, 435−447.

Holtwick, R., Meinhardt, F., Keweloh, H. 1997. *cis-trans* isomerization of unsaturated fatty acids: cloning and sequencing of the *cti* gene from *Pseudomonas putida* P8. Appl. Environ. Microbiol. 63, 4292–4297.

Hoover, W.G. 1985. Canonical dynamics: equilibrium phase-space distributions. Phys. Rev. A 31, 1695−1697.

Hyslop, P.A., Morel, B., Sauerheber, R.D. 1990. Organization and interaction of cholesterol and phosphatidylcholine in model bilayer membranes. Biochemistry. 29, 1025−1038.

Jala, R.C.R., Xu, X., Guo, Z. 2013. Enzymatic production of trans fatty acid free fat from partially hydrogenated soybean oil (PHSO) – Theory, strategy and practicability. Food Chem. 141, 1934–1940.

Jorgensen, W.L., Chandrasekhar, J., Madura, J.D., Impey, R.W., Klein, M.L., 1983. Comparison of simple potential functions for simulating liquid water. J. Chem. Phys. 79, 926–935.

Jorgensen, W.L., Maxwell, D.S., TiradoRives, J. 1996. Development and testing of the OPLS all-atom force field on conformational energetics and properties of organic liquids. J. Am. Chem. Soc. 118, 11225−11236.

Junker, F., Ramos, J. 1999. Involvement of the cis-trans isomerase Cti in the solvent resistance of *Pseudomonas putida* DOT-T1E. J. Bacteriol. 181, 5693–5700.

Kaminski, G.A., Friesner, R.A., Tirado-Rives, J., Jorgensen, W.L. 2001. Evaluation and reparametrization of the OPLS-AA force field for proteins via comparison with accurate quantum chemical calculations on peptides. J. Phys. Chem., 105, 6474−6487.

Keweloh, H., Heipieper, H.J. 1996. Trans unsaturated fatty acids in bacteria. Lipids, 31, 129–137.

Klauda, J.B., Brooks, B.R., MacKerell, A.D., Venable, R.M., Pastor, R.W. 2005. An Ab Initio study on the torsional surface of alkanes and its effect on molecular simulations of alkanes and DPPC bilayers. J. Phys. Chem. B, 109, 5300−5311.

Klauda, J.B., Garrison, S.L., Arora, G., Jiang, J., Sandler, S.I. 2004. HM-IE: A quantum Chemical hybrid method for accurate interaction energies. J. Phys. Chem. A, 108, 107–112.

Koynova, R., Caffrey, M. 1998. Phases and phase transitions of the phosphatidylcholines. Biochim. Biophys. Acta 1376, 91–145.

Krause, M.R., Wang, M., Mydock-McGrane, L., Covey, D.F., Tejada, E., Almeida, P.F., Regen S.L. 2014. Eliminating the roughness in cholesterol's β-face: does it matter? Langmuir 30, 12114–12118.

Kučerka, N., Gallová, J., Uhríková, D., Balgavý, P., Bulacu, M., Marrink, S.-J., Katsaras, J. 2009. Areas of monounsaturated diacylphosphatidylcholines. Biophys. J. 97, 1926–1932.

Kucerka, N., Tristram-Nagle, S., Nagle, J.F. 2006. Closer look at structure of fully hydrated fluid phase DPPC bilayers. Biophys. J. 90, L83–L85.

Kučerkaa, N., Nieh, M.-P., Katsaras, J. 2011. Fluid phase lipid areas and bilayer thicknesses of commonly used phosphatidylcholines as a function of temperature. Biochim. Biophys. Acta 1808, 2761-2771

Kulig, W., Tynkkynen, J., Javanainen, M., Manna, M., Rog, T., Vattulainen, I., Jungwirth, P. 2014. How well does cholesteryl hemisuccinate mimic cholesterol in saturated phospholipid bilayers? J. Mol. Model. 20, 2121 (1-9).

Larque, E., Zamora, S., Gil, A. 2001. Dietary trans fatty acids in early life: a review. Early Human Devel. 65, S31–S41.

Lingwood, D., Binnington, B., Róg, T., Vattulainen, I., Chai, W., Feizi, T., Grzybek, M., Coskun, U., Lingwood, C., Simons, K., 2011b. Cholesterol regulates glycolipid conformation, and receptor activity. Nature Chem. Biol. 7, 260–262.

Maciejewski, A., Pasenkiewicz-Gierula, M., Cramariuc, O., Vattulainen, I., Róg, T., 2014. Refined OPLS-AA force field for saturated phosphatidylcholine bilayers at full hydration. J. Phys. Chem. B 118, 4571-4581.

Magarkar, A., Dhawan, V., Kallinteri, P., Viitala, T., Elmowafy, M., Róg, T., Bunker, A. 2014. Cholesterol level affects surface charge of lipid membranes in physiological environment. Sci. Rapp. 4, 5005.

Martinez-Seara, H., Róg, T., Pasenkiewicz-Gierula, M., Vattulainen, I., Karttunen, M., Reigada, R. 2008. Interplay of unsaturated phospholipids and cholesterol in membranes: effect of double bond position. Biophys. J. 95, 3295-3305.

Mendes Ferreira, T., Coreta-Gomes, F., Ollila, O.H.S., Joao Moreno, M., Vaz, W.L.C., Topgaard, D., 2013. Cholesterol and POPC segmental order parameters in lipid membranes: solid state 1H–13C NMR and MD simulation studies. Phys. Chem. Chem. Phys. 15, 1976–1989.

Morita, N., Shibahara, A., Yamamoto, K., Shinkai, K., Kajimoto, G., Okuyama, H. 1993. Evidence for *cis-trans* isomerization of a double bond in the fatty acids of the psychrophilic bacterium *Vibrio sp.* Strain ABE-1. J. Bacteriol. 175, 916–918.

Morita, N.A., Shibahara, K., Yamamoto, K., Shinkai, G., Kajimoto, G., Okuyama, H. 1993. Evidence for *cis-trans* isomerization of a double bond in the fatty acids of the psychrophilic bacterium *Vibrio* sp. strain ABE-1. J. Bacteriol. 175, 916–918

Moss, R.A., Fujita, T., Okumura, Y. 1991. Effect of unsaturation on lipid dynamics within synthetic lipid membranes Langmuir, 7, 440–441.

Murzyn, K., Róg, T., Jezierski, G., Kitamura, K., Pasenkiewicz-Gierula, M. 2001. Effects of phospholipid unsaturation on the membrane/water interface: a molecular simulation study. Biophys. J. 81, 170-183.

Niu, S-L., Mitchell, D.C., Litman B.J. 2005. Trans fatty acid derived phospholipids show increased membrane cholesterol and reduced receptor activation as compared to their *cis* analogs. Biochemistry 44, 4458–4465

Nose, S. 1984. A unified formulation of the constant temperature molecular dynamics methods. J. Chem. Phys. 81, 511−519.

Ohnishi, M., Thompson, Jr. G. A. 1991. Biosynthesis of the unique *trans*-_3-hexadecenoic acid component of chloroplast phosphatidylglycerol: evidence concerning its site and mechanism of formation. Arch. Biochem. Biophys. 288, 591–599.

Ohvo-Rekilä, H., Ramstedt, B., Leppimäki, P., Slotte, J.P. 2002. Cholesterol interactions with phospholipids in membranes. Prog. Lipid Res. 41, 66–97.

Okuyama, H., Okajima, N., Sasaki, S., Higashi, S., Murata, N. 1991. The *cis/trans* isomerization of the double bond of a fatty acid as a strategy for adaptation to changes in ambient temperature in the psychrophilic bacterium, *Vibrio sp.* strain ABE-1. Biochim. Biophys. Acta 1084, 13–20.

Parrinello, M., Rahman, 1981. A. polymorphic transitions in single crystals: A new molecular dynamics method. J. Appl. Phys. 52, 7182−7190.

Pasenkiewicz-Gierula, M., Takaoka, Y., Miyagawa, H., Kitamura, K., Kusumi, A. 1999. Charge pairing of headgroups in phosphatidylcholine membranes: a molecular dynamics simulation study. Biophys. J. 76, 1228-1240.

Pearce, L.L., Harvey, S.C. 1993. Langevin dynamics studies of unsaturated phospholipids in a membrane environment. Biophys. J. 65, 1084–1092.

Plesnar, E., Subczynski, W.K., Pasenkiewicz-Gierula M., 2013. Comparative computer

simulation study of cholesterol in hydrated unary and binary lipid bilayers and in an anhydrous crystal. J. Phys. Chem. B 117, 8758-8769.

Roach, C., Feller, S.E., Ward, J.A., Shaikh, S.R., Zerouga, M., Stillwell, W. 2004. Comparison of *cis* and *trans* fatty acid containing phosphatidylcholines on membrane properties.| Biochemistry**,** 43, 6344–6351

Róg T., Vattulainen, I. 2014. Cholesterol, sphingolipids, and glycolipids: What do we know about their role in raft-like membranes. Chem. Phys. Lipids 184, 82–104.

Róg, T., Murzyn, K., Gurbiel, R., Kitamura, K., Kusumi, A., Pasenkiewicz-Gierula, M. 2004. Effects of phospholipid unsaturation on the structure and dynamics of the hydrocarbon core of the membrane. A molecular simulation study. J. Lip. Res. 45, 326–336.

Róg, T., Pasenkiewicz-Gierula, M. 2004. Cholesterol-phospholipid hydrophobic interactions: a molecular simulation study. Biophys. Chem. 107, 151-164.

Róg, T., Pasenkiewicz-Gierula, M., 2003. Comparison of effects of epicholesterol and cholesterol on the phosphatidylcholine bilayer: A molecular dynamics simulation study. Biophys. J. 84, 1818-1826.

Róg, T., Pasenkiewicz-Gierula, M., Vattulainen, I., Karttunen, M. 2009. Ordering effects of cholesterol and its analogues. Biochim. Biophys. Acta 1788, 97–121.

Róg, T., Vattulainen, I. 2014. Cholesterol, sphingolipids, and glycolipids: What do we know about their role in raft-like membranes. Chem. Phys. Lipids, 184:82-104.

Róg, T., Vattulainen, I., Pasenkiewicz-Gierula, M., Karttunen, M., 2007. What happens if cholesterol is made smoother: Importance of methyl substituents in cholesterol ring structure on phosphatidylcholine-sterol interaction. Biophys. J. 92, 3346-3357.

Sardessa, Y., Bhosle, S. 2002. Tolerance of bacteria to organic solvents. Res. Microbiol. 153, 263–268.

Schofield, C.R., Davison, V.L., Dutton, H.J. 1967. Analysis for geometrical and positional isomers of fatty acids in partially hydrogenated fats. J. Am. Oil. Chem. Soc. 44, 648–651.

Segura A., Molina, L., Fillet, S., Krell, T., Bernal, P., Munoz-Rojas J., Ramos, J-L. 2012. Solvent tolerance in Gram-negative bacteria. Curr. Opinion Biotech. 23, 415–421

Seelig, J., Waespe-Sarcevit, N. 1978. Molecular order in cis and trans unsaturated phospholipid bilayers. Biochemistry 317, 310-3315.

Shivaji Jogadhenu, S., Prakash, S.S. 2010. How do bacteria sense and respond to low temperature? Arch. Microbiol. 192, 85–95.

Song, Y., Kenworthy, A.K., Sanders, C.R. 2014. Cholesterol as a co-solvent and a ligand for membrane proteins. Protein Sci. 23, 1–22.

Soni, S.P., Ward, J.A., Sen, S.E., Feller, S.E., Wassall, S.R. 2009. Effect of trans unsaturation on molecular organization in a phospholipid membrane. Biochemistry 48, 11097–11107.

Stephenson, R.M., Malanowski, S. Eds. 1987. Handbook of the thermodynamics of organic compounds. Elsevier.

Stępniewski, M., Kepczynski, M., Jamróz, D., Nowakowska, M., Rissanen, S., Vattulainen, I., Róg, T. 2012. Interaction of hematoporphyrin with lipid bilayer. Molecular dynamics simulation studies. J. Chem. Phys. B, 116, 4889−4897.

Subczynski, W.K.J., Hyde, J.S**.,** Kusumi, A. 1991. Effect of alkyl chain unsaturation and cholesterol intercalation on oxygen transport in membranes: A pulse ESR spin labeling study? Biochemistry 30**,** 8578–8590

Torres, S., Pandey, A., Castro, G.R. 2011. Organic solvent adaptation of Gram positive bacteria: Applications and biotechnological potentials. Biotech. Adv. 29, 442–452.

Uauy, R., Aro, A., Clarke, R., Ghafoorunissa, R.,Abbe, M.L., Mozaffarian, D., Skeaff, M., Stender, S., Tavella, M. 2009. WHO Scientific Update on trans fatty acids: summary and conclusions. Eur. J. Clinic. Nutrition 63, S68–S75.

Waarts, B.L., Bittman, R., Wilschut, J., 2002. Sphingolipid and cholesterol dependence of alphavirus membrane fusion. Lack of correlation with lipid raft formation in target liposomes, J. Biol. Chem. 277, 38141–38147.

van Tol, A., Zock, P.L., van Gent, T., Scheek, L.M., Katan, M.B. 1995. Dietary *trans* fatty acids increase serum cholesterylester transfer protein activity in man. Atherosclerosis 115, 129–134.

Weber, F,. Isken, S., de Bont, J. 1994. Cis-trans isomerisation of fatty acids as a defence mechanism of *Pseudomonas putida* S12 to toxic concentrations of toluene. Microbiol. 140, 2013–2017.

Vollhardt, D. 2007. Effect of unsaturation in fatty acids on the main characteristics of Langmuir monolayers. J Phys. Chem. C, 111, 6805–6812.

Yaws, C.L. Ed. 2009. Thermophysical properties of chemicals and hydrocarbons, Elsevier.